ACS OMEGA

Open Access

http://pubs.acs.org/journal/acsodf

Article

Comparative Investigation of AquaSun Eco-Friendly Antifouling Coating via Rheological and Mechanical Characterization

Cristina Scolaro,* Silvia Sfameni, Mario Pagliaro,* Rosaria Ciriminna,* and Annamaria Visco*

Cite This: *ACS Omega* 2023, 8, 43850−43855

Read Online

ACCESS | Metrics & More | Article Recommendations

ABSTRACT: Rheological and mechanical comparative tests of the new AquaSun antifouling sol−gel coating coated on shipbuilding steel compared to a commercial silyl acrylate antifouling top coat containing cuprous oxide and copper pyrithione show further evidence of the practical viability of this multifunctional coating for the protection of the immersed surfaces from biofouling. AquaSun is a less rigid or less viscous material than commercial top coat but more adherent to the steel substrate. These results support further investigation of this multifunctional sol−gel coating as an eco-friendly antifouling paint.

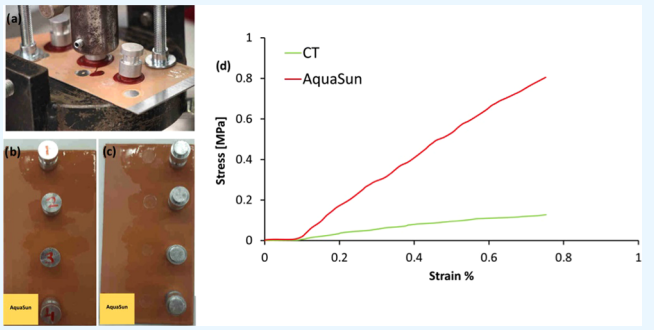

1. INTRODUCTION

Today chiefly based on "self-polishing" copolymer paints containing cuprous oxide (Cu_2O) as the main biocide often in combination with other biocidal species to broaden the spectrum of action against the widely different organisms (barnacles, mussels, algae, dog teeth, etc.) comprising marine biofouling, antifouling (AF) paints are applied to commercial and recreational vessels at 100,000 t/a yearly rate.[1,2] Over 3−5 years, the AF coating applied to the vessel's hull releases all Cu^+ and booster biocides into seawater significantly impacting marine life including coastal macrofouling communities.[3,4] The leached biocides, indeed, are poorly biodegradable and therefore remain in marine sediments for a long time, harming the aquatic environment.[5−7]

Numerous new "green" commercial AF paints exist.[7,8] Yet, most of them are significantly more expensive than conventional biocidal antifouling coatings.[9,7] Xerogels of organically modified silica (ORMOSIL) are the most recently commercialized eco-friendly foul release (FR) coatings.[10] Likewise to much thicker silicone-based FR coatings, these top coats act by minimizing the surface energy of the protected hull, thereby reducing the initial stages of fouling development and easing the removal of the fouling network that accumulates during the vessel motion.[11] Unfortunately, these biocide-free FR coatings exert little antifouling function when the vessel is stationary, such as in port waters or during idling, and generally underperform in warm marine waters with water temperatures above 25 °C.

AquaSun is a new ORMOSIL-based antifouling coating functionalized with flower-like microparticles of visible-light photocatalyst Bi_2WO_6, which merges the solar-driven photocatalytic generation of powerful oxidizing species H_2O_2 and hydroxyl radicals that readily degrade biomolecules and microbiological species, with the FR properties of conventional ORMOSIL xerogels.[12,13] Composed of a thin ORMOSIL film encapsulating the aforementioned visible-light photocatalyst, the coating also shows high strength of adhesion to real ship steel substrates and complete lack of ecotoxicity.[14] Recent comparative tests carried out for 3 months, furthermore, unveiled the AF activity of AquaSun even in highly polluted port seawaters for prolonged time under stationary condition of the coated shipbuilding steel substrates.[15]

To further demonstrate the practical applicability of this new multifunctional (AF/FR) coating, in this study, we report the outcomes of rheological (through dynamic stress sweep test, amplitude sweep test, and temperature sweep tests) and mechanical (through cross-cut test and pull-off test) characterization aimed at evaluating the adhesive and rheological properties of the AquaSun top coat compared to a commercial top coat. Adhesion to shipbuilding steel is a crucial feature for the effectiveness of both FR and AF paints. The rheological properties of paints and coatings, in turn, crucially impact the application and subsequent behavior of paints. To ensure optimal deposition and avoid sagging or casting, for example, the rheological parameter of viscosity should be of intermediate value, namely, not too high nor too low.[16,17]

Received: August 7, 2023
Accepted: September 21, 2023
Published: November 7, 2023

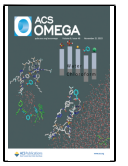

Knowledge of the rheological behavior of a coating at different shear rates, furthermore, is important for the design of the equipment required for the application of such coatings.[18−20]

2. MATERIALS AND METHODS

2.1. Coating Preparation and Characterization. The preparation and application of the AquaSun coating takes place via a three-step process. Starting from a formulation incorporating 12% w/w of Bi_2WO_6 suspended in a C18 1%/C8 49%/TEOS 50% silane solution in 2-propanol (wherein C18 stands for *n*-octadecyltrimethoxysilane, C8 for *n*-octyltriethoxysilane, and TEOS for tetraethylorthosilicate), the preparation of AquaSun via hydrolytic sol−gel polycondensation under acidic conditions is described in detail elsewhere.[14] The resulting waterborne paint was deposited on the shipbuilding steel surface via simple brushing followed by curing at room temperature. The commercial top coat, a silyl acrylate antifouling coating (SeaQuantum Ultra S, containing 785 g/L copper(I) oxide and 66 g/L copper pyrithione),[21] was purchased from Jotun (Sandefjord, Norway) and similarly applied to shipbuilding steel with a brush.

2.2. Rheological and Mechanical Characterization. The flow behavior of liquidlike samples at room temperature was analyzed through a rotational rheometer (MC-502, Anton Paar, Graz, Austria) consisting of a rotating rod immersed in the liquid to be analyzed. The terminal part of the rod had a specific shape (geometry). Measurements for this study were carried out by using cone−plate geometry. For each geometry, the lower support was always fixed (only the upper part was connected to the motor moves). A dynamic stress sweep test was performed to check the linear viscoelastic region (LVR). This region was checked by an amplitude sweep test of the top coats CT (commercial coating) and AquaSun at room temperature (25 °C) and at a constant 1 Hz frequency within the 0.001 up to 10,000 s^{-1} stress interval. From the said test, the 56 Pa stress value was selected. The temperature sweep test (at a constant stress value of 56 Pa) was conducted in the 25−180 °C thermal interval. Decreasing continuously the duration for each measurement with increasing shear rates (starting at a shear rate of 100 s^{-1} and ending at 1500 s^{-1}), the shear rate test was carried out by measuring 18 values using ascending logarithmic steps. Each test was performed 3 times.

The adhesion of coating films to DH36 shipbuilding steel (a structural grade of steel used for the construction of ships and offshore platforms) substrate was evaluated by cross-cut test and pull-off test. The cross-cut test was performed by using a commercial Cross Hatch Adhesion Tester (SAMA Tools SADT502−5 (SAMA Italia, Viareggio, Italy)) according to the ASTM D3359e2 Standard Test Method for Measuring Adhesion by Tape Test. Using an appropriate cutter, a grid incision was made in a test area of approximately 10 cm × 10 cm, creating a grid of horizontally and vertically spaced (2 mm) incisions across the surface. All particles produced in the area were then removed with a soft brush. As a rule, 3M (Maplewood, MN, USA) adhesive tape was stuck onto the cutting grid with a finger, applying light pressure, after which it was subsequently removed with an even peeling movement. The test was evaluated visually by comparing the sectional grid image with the reference images from the ISO 2409:2013 international standard. Depending on the condition of the damage, a cross-cut parameter from 0 (very good adhesive strength) to 5 (very poor adhesive strength) was assigned to each sample according to the number of squares that have flaked off and to the appearance. After complete drying of the second tie coat layer, a circular third layer with a diameter of ∼10 mm was deposited as the top coat (∼190 μm tick) beneath each metallic dolly for the pull-off test. Before adhering to the top coat, the dollies were rubbed and rinsed with a cotton swab previously immersed in EtOH followed by drying with a dry cloth. The pull-off test was carried out with a Lloyd LR10K Universal Dynamometer machine (load cell 10 kN, preload 1.00 N, speed 1 mm/min) purchased from Ametek-Lloyd Instruments (Fareham Hampshire, Great Britain) according to ASTM D4541−02 (or ISO4624:2016) standards attaching a steel metal dolly perpendicularly to a 5 mm thick DH36 steel plate having a 80 mm × 10 mm area.

A test dolly initially glued to the coating deposited in a small circular area of 1.5 mm in diameter on the metal specimens in DH36 shipbuilding steel plate previously coated with primer and tie coat was first fixed to a coupling fitting of the dynamometer and then pulled by a force perpendicular to the surface. The force with which the test dolly is removed from the support and the type of failure obtained were recorded using a stress/strain curve as a measure of the adhesion properties of the coating. The type of fracture of the dolly from the substrate was evaluated according to the aforementioned international standards. Mechanical values (Young's modulus *E*, [MPa]; stress at break, σr [MPa]; deformation at break, εr [%]; work at break, *Wr* [J]) were obtained as the result of the average values obtained from three samples (for each type) of at least four dollies. Prism 8.0.2 statistical software (GraphPad, La Jolla, CA, USA) was used for the statistical analysis. Data are reported as mean ± SD (±Standard Deviation) at a significance level of $p < 0.05$. The D'Agostino−Pearson test was used for the normality test of data, and Brown−Forsythe test was used for the homogeneity of the variance test. Since all data used in this study satisfied the latter tests, one-way analysis of variance (ANOVA) with Bonferroni's *post hoc* test was performed to evaluate the statistical significance of the differences between the groups (significance level: 0.05).

3. RESULTS AND DISCUSSION

3.1. Evaluation of the Rheological Features of the Coatings. Displaying the loss (G'', red curve) and conservative (G', black curve) modulus vs temperature curves for the commercial antifouling (CT, a) and the AquaSun (b) coatings, Figure 1 clearly shows the crossing point of each pair of curves defining the point where the resins cross-link.

The crossing point decreases from 146 °C for the commercial top coat to 105 °C for the AquaSun sol−gel coating. This shows evidence that the commercial resin cross-links at significantly higher temperatures because of its higher structural complexity compared to the AquaSun organosilica layer which cross-links at temperatures slightly exceeding 100 °C.

Revealing the organic polymer nature of the commercial top coat, its elastic conservative G' modulus is more than 3 orders of magnitude higher than that of AquaSun consisting of a glassy ORMOSIL. The higher structural complexity of the commercial top coat compared to the experimental sol−gel coating is confirmed by the complex viscosity (η^*) of the three coatings shown in Figure 2.

Below 100 °C, the value of η^* of the commercial coating is about 7×10^6 mPa x s, while that of the AquaSun coating is more than 3 orders of magnitude lower (∼1400 mPa x s for AquaSun). The gel point, i.e., the temperature at which

https://doi.org/10.1021/acsomega.3c05787
ACS Omega 2023, 8, 43850−43855

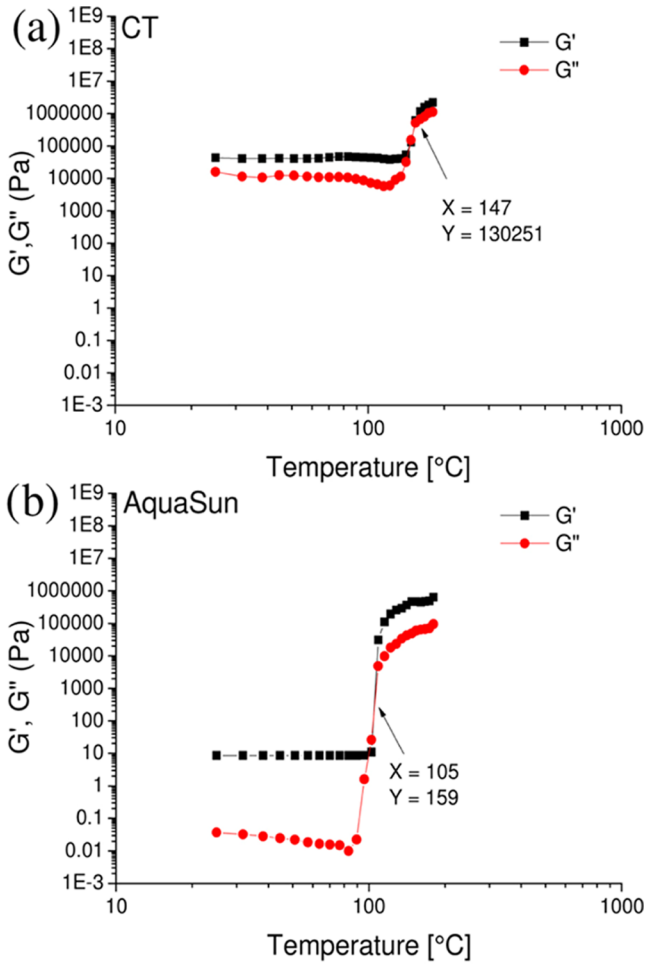

Figure 1. Thermal behavior of loss (G'') and conservative (G') moduli of SeaQuantum Ultra S commercial (CT, a) and AquaSun (b) coatings.

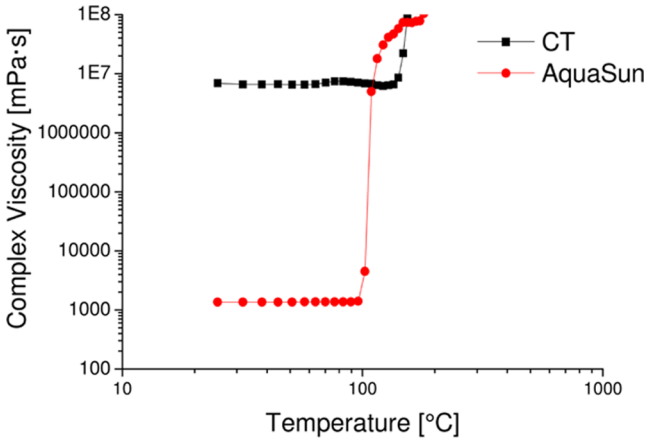

Figure 2. Thermal behavior of the complex viscosity (η^*) of SeaQuantum Ultra S commercial (CT) and AquaSun coatings.

exponential growth of viscosity is observed as the resin begins to cross-link, occurs at 103 °C, whereas it shifts to 146 °C for the commercial top coat.

The rheological behavior of the top coats (both the commercial organic polymer and AquaSun) was studied at different temperatures. The graphs in Figure 3 show the shear stress vs shear strain curves of the top coats at 25, 30, 40, 50, and 75 °C at different strain rates. The curves in Figure 3a,3b reveal rigid plastic materials. In detail, the curves in Figure 3a, closer to each other, show that the rheological behavior of the commercial polymeric coating CT is more stable when increasing the temperature compared to the organosilica thin film comprising the AquaSun coating. The latter retains good mechanical performance up to 50 °C. At 75 °C, the CT coating has a strikingly different behavior when compared to AquaSun, with the shear stress increasing, rather than decreasing, and eventually reaching the highest value amid all thermal conditions tested.

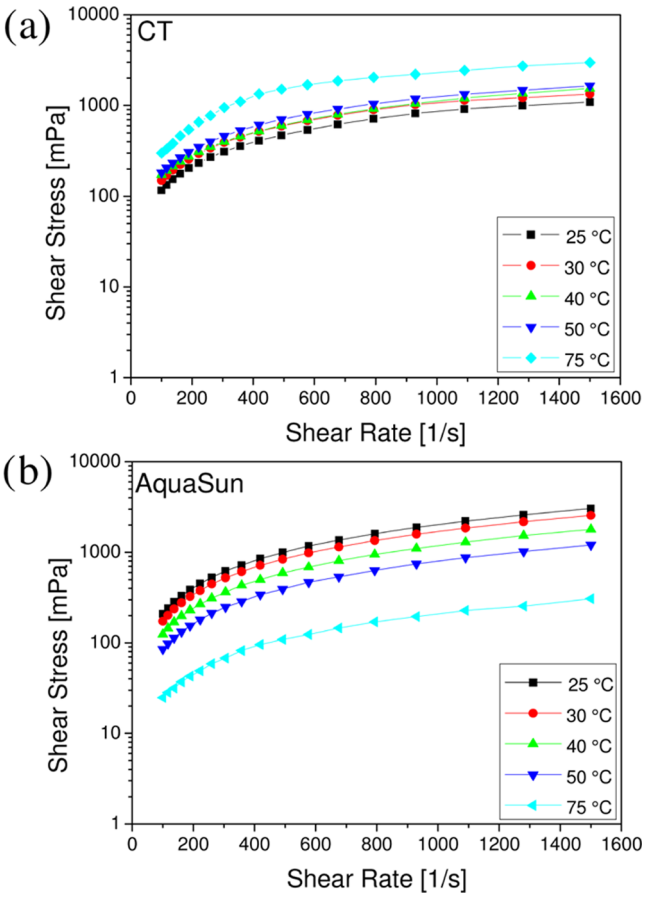

Figure 3. Shear stress vs shear strain curves of SeaQuantum Ultra S commercial (CT, a) and AquaSun (b) coatings in the 25−75 °C temperature range.

This behavior is likely due to the complete evaporation and removal of the solvent from the CT layer, leaving a rigid top coat that completely lost its initial elasticity. Indeed, after the rheological test, the CT polymer film (deposited on the rheometer plate) appeared with cracks and internally split, showing evidence of lost homogeneity. On the contrary, the robust AquaSun hybrid glassy coating retained its ductility even at the highest temperature tested (75 °C).

Figure 4, furthermore, compares the shear stress of AquaSun (containing the photocatalyst Bi_2WO_6) with the shear stress of CT coating at 75 °C. The curves show that the shear stress at the high shear rate of 1000 s^{-1}, changes by about 1 order of magnitude, going from about 2200 mPa s for the commercial coating to 195 mPa s for the AquaSun top coat. Similarly, in Figure 5 the viscosity curves confirm the trend of the shear stress because the viscosity of the CT increases with the temperature whereas that of AquaSun decreases. At 75 °C the

https://doi.org/10.1021/acsomega.3c05787
ACS Omega 2023, 8, 43850−43855

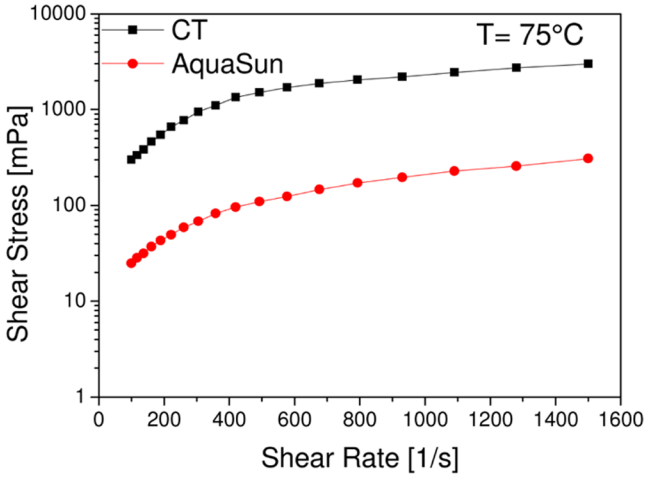

Figure 4. Shear stress vs shear strain of SeaQuantum Ultra S commercial (CT) and AquaSun coatings at 75 °C.

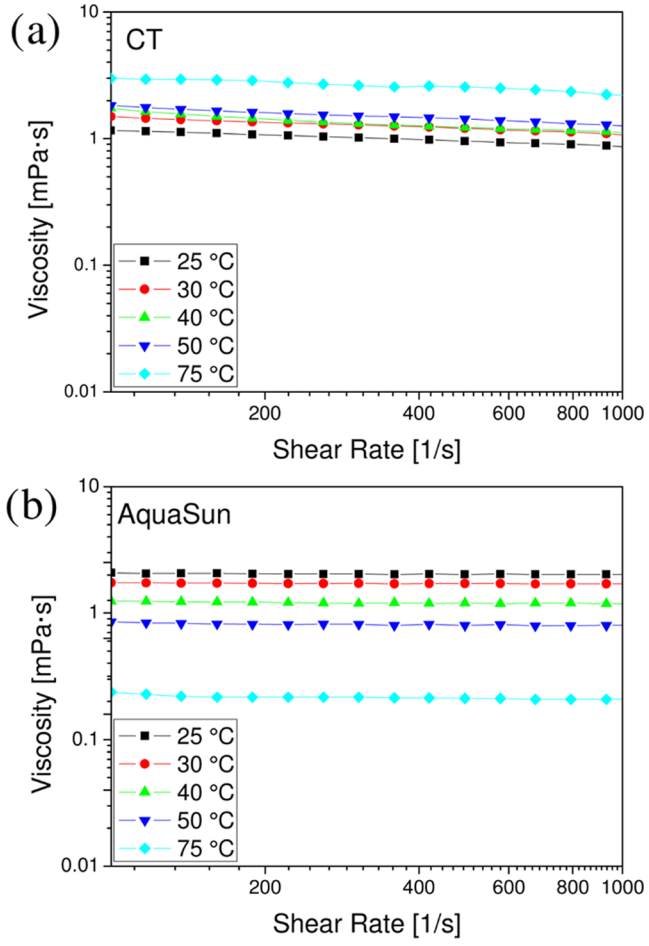

Figure 5. Viscosity vs shear strain of commercial SeaQuantum Ultra S commercial (CT, a) and AquaSun (c) coatings at different temperatures within the 25−75 °C range.

viscosity of CT at the shear rate of 1000 s^{-1} is about 2 mPa s while that of AquaSun is about 0.2 mPa s, according to data in Figure 3. This shows evidence that the AquaSun coating has a lower viscosity and is significantly softer when compared to CT reference coating.

3.2. Evaluation of the Adhesion Power of the Coatings. The outcomes of the cross-cut and pull-off mechanical tests used to evaluate the adhesion power of the coatings are displayed in Figure 6. The optical microscopy photographs therein suggest a different morphology of the reference sample (CT), which is opaque compared to the glossy appearance of the AquaSun vitreous coatings.

To better observe the effects of adhesion strength on the metallic substrate, optical microscopic photographs of the cut area were taken at 50× and 400× magnification on each sample. The CT reference sample showed a grid in which the cutting edge descends to the bottom of the coatings, unveiling the gray color of the primer, while the tie coat is distributed on the lateral sides of each groove left by the cutter. On the other hand, the lateral redistribution of the antifouling top coat was less visible in the substrate coated with AquaSun where the gray primer substrate was significantly less evident. Hence, it may be concluded that the AquaSun top coat has a better adhesive power than the commercial top coat. The stress−strain curves of the adhesive adhesion power of AqauSun and the commercial finish in Figure 7d showing the outcomes of the pull-off adhesion test clearly reveal the substantially stronger adhesion of the AquaSun sol−gel coating in comparison to the polymeric commercial antifouling paint.

Visual examination of the relevant adhesion area for each coating after the rupture of the adhesive layer between the coating and the coated dolly also clearly reveals that AquaSun exhibits the highest mechanical adhesion (Figure 7c). The main mechanical parameters for the commercial and AquaSun coatings are listed in Table 1.

Statistical analysis confirmed that the mechanical parameters of the pull-off test of the coatings were statistically highly significant for all samples ($p < 0.0001$). As mentioned above, the AquaSun top coat showed better adhesion than the commercial coating. In detail, the commercial paint showed a modest percentage elongation ($\varepsilon r\% = 0.75$) reaching the yield point, and therefore plastic deformation, with a stress of only 0.14 MPa ($p < 0.0001$). The AquaSun coating had the same percentage of deformation at break ($\varepsilon r\% = 0.75$) but at a tensile strength of 0.81 MPa ($p < 0.0001$), namely, which is reflected in a work at break enhancement growing from ∼9 N for the commercial paint to ∼61 N ($p < 0.0001$) for the AquaSun sol−gel coating. Finally, the Young's modulus improved by more than 4 times, going from ∼30 MPa for the commercial polymeric antifouling paint to ∼130 MPa ($p < 0.0001$) for the AquaSun coating.

4. OUTLOOK AND CONCLUSIONS

The results of the first rheological and mechanical comparative analyses carried out on the new AquaSun antifouling sol−gel coating clearly show that AquaSun is a less rigid and less viscous material than a state-of-the-art commercial antifouling top coat but substantially more adherent to shipbuilding steel substrate. The reason is linked to its lower viscosity and lower stiffness thanks to which the glassy organosilica sol containing plentiful Si−OH groups is able to chemically bind to the Fe−OH groups at the steel surface eventually affording a strongly cohesive thin film.[22] Such a thin film is ideally suited to coat and protect the outer steel surface not only from corrosion[23] but also from biofouling.

Involving rapid microbial surface colonization followed by biofilm development and eventually attachment of large and hard marine organisms,[24] marine biofouling of submerged objects such as boat or ship hulls and pier pylons is a biological colonization process causing significant economic losses

https://doi.org/10.1021/acsomega.3c05787
ACS Omega 2023, 8, 43850−43855

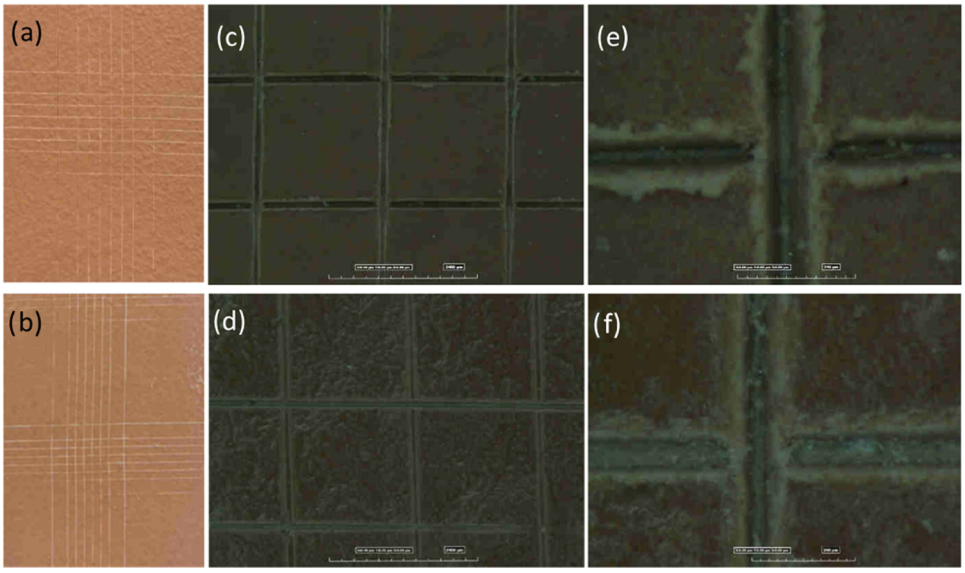

Figure 6. Optical microscopy photographs of the cross-cut test grid in commercial SeaQuantum Ultra S (a) and AquaSun (b) coatings at 50× (c, d) and 400× (e, f) magnification.

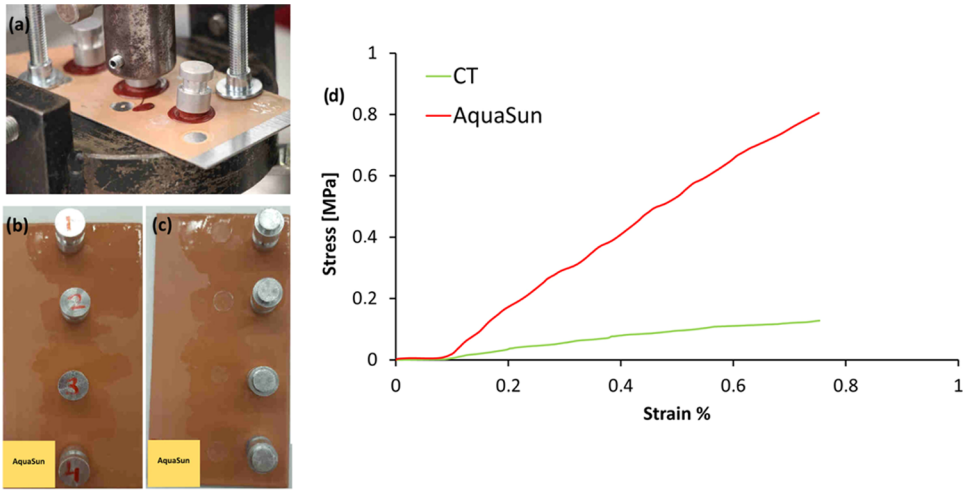

Figure 7. Pull-off test: fixing phase of the dolly in the dynamometer (a); images of the metal specimen and the dolly before and after the pull-off test for AquaSun (b, c) sample; stress/strain curves of SeaQuantum Ultra S commercial (CT) and AquaSun coatings (d).

Table 1. Mechanical Parameters of Commercial SeaQuantum Ultra S (CT) and AquaSun Coatings

sample	E (MPa)	σr (MPa)	εr (%)	Lr (N)	Wr (J)
CT	29.98 ± 1.08	0.14 ± 0.07	0.75 ± 0.05	9.75 ± 0.52	0.0004 ± 0.0001
AquaSun	130.42 ± 1.61	0.81 ± 0.05	0.75 ± 0.08	61.76 ± 0.57	0.0022 ± 0.0001

worldwide. The new photocatalytic AquaSun coating combines the foul release properties of the organosilica with the photocatalytic generation of H_2O_2 and hydroxyl radicals driven by sunlight that prevent microbial colonization and biofilm deposition.[12,13] The powerful biocidal hydrogen peroxide generated *in situ* readily decomposes into O_2 and H_2O eventually posing no harm to the marine environment.[25]

A "triple bottom line" sustainability analysis of AquaSun production and commercial uptake recently concluded that the technology has significant potential toward replacing conventional antifouling coatings with a single product of broad applicability.[26] Besides proof of prolonged activity first in coated surfaces at sea,[15] and then in real vessels and offshore platforms in open marine waters, what is required for practical utilization of this new coating are good rheological and mechanical properties. The outcomes of this work, thus, contribute an additional important step toward practical utilization of this new eco-friendly antifouling coating. Further applications of AquaSun against biofouling on different surfaces in contact with water or moisture can be anticipated.

■ ASSOCIATED CONTENT

Data Availability Statement

All data are available upon reasonable request by contacting the corresponding authors.

https://doi.org/10.1021/acsomega.3c05787
ACS Omega 2023, 8, 43850−43855

AUTHOR INFORMATION

Corresponding Authors

Cristina Scolaro − *Dipartimento di Ingegneria, Università di Messina, 98166 Messina, Italy*; Email: cristina.scolaro@unime.it

Mario Pagliaro − *Istituto per lo Studio dei Materiali Nanostrutturati, CNR, 90146 Palermo, Italy*; orcid.org/0000-0002-5096-329X; Email: mario.pagliaro@cnr.it

Rosaria Ciriminna − *Istituto per lo Studio dei Materiali Nanostrutturati, CNR, 90146 Palermo, Italy*; Email: rosaria.ciriminna@cnr.it

Annamaria Visco − *Dipartimento di Ingegneria, Università di Messina, 98166 Messina, Italy; Istituto per i Polimeri, Compositi e Biomateriali, CNR, 95126 Catania, Italy*; Email: annamaria.visco@unime.it

Author

Silvia Sfameni − *Dipartimento di Ingegneria, Università di Messina, 98166 Messina, Italy*

Complete contact information is available at: https://pubs.acs.org/10.1021/acsomega.3c05787

Notes

The authors declare no competing financial interest.

ACKNOWLEDGMENTS

The authors thank NAVTEC (Consorzio di Ricerca per l'Innovazione tecnologica, Sicilia, Trasporti navali, commerciali e da diporto s.c.a.r.l) for research funding, grant number ARS01_00293 PON2014-2020 of research project "Thalassa" (TecHnology And materials for safe Low consumption and low life cycle cost veSSels And crafts). Thanks to Giuseppe Napoli, Istituto per lo Studio dei Materiali Nanostrutturati, CNR, for administrative assistance.

REFERENCES

(1) Paz-Villarraga, C. A.; Castro, Í. B.; Fillmann, G. Biocides in antifouling paint formulations currently registered for use. *Environ. Sci. Pollut. Res.* **2022**, *29*, 30090−30101.

(2) Yebra, D. M.; Kiil, S.; Dam-Johansen, K. Antifouling technology - past, present and future steps towards efficient and environmentally friendly antifouling coatings. *Prog. Org. Coat.* **2004**, *50*, 75−104.

(3) Cima, F.; Varello, R. Potential disruptive effects of copper-based antifouling paints on the biodiversity of coastal macrofouling communities. *Environ. Sci. Pollut. Res.* **2023**, *30*, 8633−8646.

(4) Torres, F. G.; De-la-Torre, G. E. Environmental pollution with antifouling paint particles: Distribution, ecotoxicology, and sustainable alternatives. *Mar. Pollut. Bull.* **2021**, *169*, No. 112529.

(5) Baker, T. J.; Tyler, C. R.; Galloway, T. S. Impacts of metal and metal oxide nanoparticles on marine organisms. *Environ. Pollut.* **2014**, *186*, 257−271.

(6) Srinivasan, M.; Swain, G. W. Managing the use of copper-based antifouling paints. *Environ. Manage.* **2007**, *39*, 423−441.

(7) Ciriminna, R.; Bright, F. V.; Pagliaro, M. Ecofriendly antifouling marine coatings. *ACS Sustainable Chem. Eng.* **2015**, *3*, 559−565.

(8) (a) Silva, E. R.; Ferreira, O.; Ramalho, P. A.; Azevedo, N. F.; Bayón, R.; Igartua, A.; Bordado, J. C.; Calhorda, M. J. Eco-friendly non-biocide-release coatings for marine biofouling prevention. *Sci. Total Environ.* **2019**, *650*, 2499−2511. (b) Lagerström, M.; Wrange, A.-L.; Oliveira, D. R.; Granhag, L.; Larsson, A. I.; Ytreberg, E. Are silicone foul-release coatings a viable and environmentally sustainable alternative to biocidal antifouling coatings in the Baltic Sea region? *Mar. Pollut. Bull.* **2022**, *184*, No. 114102.

(9) Dobretsov, S.; Thomason, J. C. The development of marine biofilms on two commercial non-biocidal coatings: A comparison between silicone and fluoropolymer technologies. *Biofouling* **2011**, *27*, 869−880.

(10) Detty, M. R.; Ciriminna, R.; Bright, F. V.; Pagliaro, M. Environmentally benign sol-gel antifouling and foul-releasing coatings. *Acc. Chem. Res.* **2014**, *47*, 678−687.

(11) Detty, M. R.; Ciriminna, R.; Bright, F. V.; Pagliaro, M. Xerogel coatings produced by the sol-gel process as anti-fouling, fouling release surfaces: From lab bench to commercial reality. *ChemNanoMat* **2015**, *1*, 148−154.

(12) Scandura, G.; Ciriminna, R.; Xu, Y.-J.; Pagliaro, M.; Palmisano, G. Nanoflower-like Bi_2WO_6 encapsulated in ORMOSIL as a novel photocatalytic antifouling and foul-release coating. *Chem.- Eur. J.* **2016**, *22*, 7063−7067.

(13) (a) Scandura, G.; Ciriminna, R.; Ozer, L. Y.; Meneguzzo, F.; Palmisano, G.; Pagliaro, M. Antifouling and photocatalytic antibacterial activity of the AquaSun coating in seawater and related media. *ACS Omega* **2017**, *2*, 7568−7575. (b) Crisafi, F.; Pagliaro, M.; La Spada, G.; La Cono, V.; Lo Cono, V.; Marturano, L.; Scolaro, C.; Smedile, F.; Smedile, F.; Visco, A.; Visco, A.; Ciriminna, R. Antibacterial properties of AquaSun sol-gel coating. *Adv. Eng. Mater.* **2023**, No. 2300626.

(14) Scurria, A.; Scolaro, C.; Sfameni, S.; Di Carlo, G.; Pagliaro, M.; Visco, A.; Ciriminna, R. Towards AquaSun practical utilization: strong adhesion and lack of ecotoxicity of solar-driven antifouling sol-gel coating. *Prog. Org. Coat.* **2022**, *165*, No. 106771.

(15) Ciriminna, R.; Vacante, S.; Scurria, A.; Di Carlo, G.; Pagliaro, M.; Visco, A. Comparative analysis of AquaSun sol-gel coating and commercial antifouling paint in protecting shipbuilding steel in port seawaters. *Gen. Chem.* **2023**, *9*, No. 20230001.

(16) Branca, C.; Crupi, C.; D'Angelo, G.; Khouzami, K.; Rifici, S.; Visco, A.; Wanderlingh, U. Effect of montmorillonite on the rheological properties of dually crosslinked guar gum-based hydrogels. *J. Appl. Polym. Sci.* **2015**, *132*, No. 41373.

(17) Bhavsar, R.; Shreepathi, S. Evolving empirical rheological limits to predict flow-levelling and sag resistance of waterborne architectural paints. *Prog. Org. Coat.* **2016**, *101*, 15−23.

(18) Mihelčič, M.; Gunde, M. K.; Perše, L. S. Rheological behavior of spectrally selective coatings for polymeric solar absorbers. *Coatings* **2022**, *12*, No. 388.

(19) Hester, R. D.; Squire, D. R. Rheology of waterborne coatings. *J. Coat. Technol.* **1997**, *69*, 109−114.

(20) Sacks, M. D.; Sheu, R. S. Rheological properties of silica sol-gel materials. *J. Non-Cryst. Solids* **1987**, *92*, 383−396.

(21) Environmental Protection Authority. Decision. SeaQuantum Ultra S, 2015. https://www.epa.govt.nz/assets/FileAPI/hsno-ar/APP202374/5e37833476/APP202374-APP202374-Decision-document-09.04.2015.pdf (accessed September 6, 2023).

(22) Ciriminna, R.; Fidalgo, A.; Palmisano, G.; Ilharco, L. M.; Pagliaro, M. Silica-Based Sol-Gel Coatings: A Critical Perspective From A Practical Viewpoint. In *Biobased and Environmentally Benign Coatings*; Tiwari, A.; Soucek, M. D., Eds.; Scrivener Publishing: Salem (MA), 2016. pp 149−158.

(23) Dave, B. C.; Hu, X.; Devaraj, Y.; Dhali, S. K. Sol-gel-derived corrosion-protection coatings. *J. Sol−Gel Sci. Technol.* **2004**, *32*, 143−147.

(24) Dang, H.; Lovell, C. R. Microbial surface colonization and biofilm development in marine environments. *Microbiol. Mol. Biol. Rev.* **2016**, *80*, 91−138.

(25) Olsen, S. M.; Kristensen, J. B.; Laursen, B. S.; Pedersen, L. T.; Dam-Johansen, K.; Kiil, S. Antifouling effect of hydrogen peroxide release from enzymatic marine coatings: Exposure testing under equatorial and Mediterranean conditions. *Prog. Org. Coat.* **2010**, *68*, 248−252.

(26) Ciriminna, R.; Scurria, A.; Pagliaro, M. Sustainability evaluation of AquaSun antifouling coating production. *Coatings* **2022**, *12*, No. 1034.